University of Groningen

Comparison of Targeted Mass Spectrometry Techniques With an Immunoassay

Güzel, Coșkun; Govorukhina, Natalia I; Stingl, Christoph; Dekker, Lennard J M; Boichenko, Alexander; van der Zee, Ate G J; Bischoff, Rainer; Luidert, Theo M

IMPORTANT NOTE: You are advised to consult the publisher's version (publisher's PDF) if you wish to cite from it. Please check the document version below.

Document Version
Publisher's PDF, also known as Version of record

[Link to publication in University of Groningen/UMCG research database](#)

Comparison of Targeted Mass Spectrometry Techniques with an Immunoassay: A Case Study for HSP90α

*Coşkun Güzel, Natalia I. Govorukhina, Christoph Stingl, Lennard J. M. Dekker,
Alexander Boichenko, Ate G. J. van der Zee, Rainer P.H. Bischoff, and Theo M. Luider**

Purpose: The objective of this study is to better understand factors governing the variability and sensitivity in SRM and PRM, compared to immunoassay. **Experimental design:** A 2D-LC–MS/MS-based SRM and PRM assay is developed for quantitative measurements of HSP90α in serum. Forty-three control sera are compared by SRM, PRM, and ELISA following the manufacturer's instructions. Serum samples are trypsin-digested and fractionated by strong cation exchange chromatography prior to SRM and PRM measurements. Analytical parameters such as linearity, LOD, LOQ, repeatability, and reproducibility of the SRM, PRM, and ELISA are determined. **Results:** PRM data obtained by high-resolution MS correlate better with ELISA measurements than SRM data measured on a triple quadrupole mass spectrometer. While all three methods (SRM, PRM, and ELISA) are able to quantify HSP90α in serum at the ng mL^{-1} level, the use of PRM on a high-resolution mass spectrometer reduces variation and shows comparable sensitivity to immunoassay.
Conclusions and clinical relevance: Using fractionation, it is possible to measure ng mL^{-1} levels of HSP90α in a reproducible, selective, and sensitive way using PRM in serum. This opens up the possibility to use PRM in a multiplexed way as an attractive alternative for immunoassays without the use of antibodies or comparable binders.

1. Introduction

Targeted proteomics by SRM on triple quadrupole mass spectrometers is a widely used strategy to quantify multiple proteins

Drs C. Güzel, Drs C. Stingl, Dr. L. J. M. Dekker, Dr. T. M. Luider
Department of Neurology
Neuro-Oncology
Clinical and Cancer Proteomics Laboratory
Erasmus University Medical Centre
Rotterdam, The Netherlands
E-mail: t.luider@erasmusmc.nl
Dr. N. I. Govorukhina, Dr. A. Boichenko, Prof. R. P. H. Bischoff
Department of Analytical Biochemistry
Centre for Pharmacy
University of Groningen
Groningen, The Netherlands
Prof. A. G. J. van der Zee
Department of Gynecology
University Medical Centre Groningen
Groningen, the Netherlands

in complex body fluids like serum.[1–3] While SRM is a highly selective method, interferences in complex biological samples often limit sensitivity in comparison to immunoassays unless appropriate sample preparation is performed.[4–6] Co-eluting peptides with a precursor ion mass close to the peptide of interest may result in fragment ions that overlap with the targeted transitions resulting in considerable chemical noise. Such noise limits sensitivity and contributes to diminished accuracy and precision. While SRM has emerged as the most widely used experimental approach to quantify proteins in biological samples by MS,[7,8] it is nevertheless challenging to quantify low levels of proteins in biological samples like serum or plasma due to the limited loading capacity of capillary or nano-LC columns and to the often insufficient resolution needed to separate interfering compounds. This is the reason that ligand binding assays and notably ELISA are routinely used for protein bioanalysis despite their limitations such as the high development cost for sensitive, well-characterized antibodies, and cross-reactivity with other proteins or interference from other ligands binding to the target protein.[9] Advantages of the immunoassay technology are the high sensitivity (detection limits < 1 ng mL^{-1})[10] and the ease with which they can be performed in a high-throughput format. While multiplexing is possible with immunoassays, for example those based on flow cytometry, analytical quality generally suffers.[11] PRM using high-resolution MS[12] goes beyond SRM in that it covers a wider dynamic concentration range and provides data with higher mass accuracy (ppm- to sub-ppm level) thus reducing interferences caused by co-eluting compounds with similar but not identical mass transitions.[12,13] Moreover, PRM methods for individual peptides are easier to set up, since all transitions are monitored and optimal transitions can be retrieved and combined in a post-analysis way.[14] Literature on PRM shows the feasibility of the approach for quantification of proteins in complex biological samples after proteolytic digestion.[13,15,16] Notably Domon and coworkers published on the use of PRM in large-scale experiments.[17–21] However, reaching the ng mL^{-1} level in body fluids without using affinity binders (e.g. immunoglobulins) remains a challenge. This study

**ADVANCED
SCIENCE NEWS**

www.advancedsciencenews.com

**Proteomics
Clinical Applications**

www.clinical.proteomics-journal.com

Clinical Relevance

We compared concentrations of HSP90α by SRM and PRM with a commercially available and frequently used immunoassay. SRM and PRM have both the possibility to measure proteins in a multiplexed way in complex samples without the use of antibodies and other types of specific binders. A separation (e.g. SCX fractionation) that can also be performed by automation is necessary to reduce ion suppression and the effect of interfering compounds. It is concluded that notably PRM that makes use of high resolution MS reaches sensitivity comparable with the immunoassay (ng mL^{-1}). For PRM even a better reproducibility was observed compared to the immunoassay. This opens ways to address in a multiplexed manner complex samples such as serum for quantitative analysis of dozens of proteins in a single run using a relatively small volume of serum (7 μL as used in present study). The present study addresses a medical need to measure sets of proteins for which no antibodies or partly characterized antibodies are available and if the amount of serum sample is limited, for instance in population studies.

shows the feasibility to measure low protein levels (ng mL^{-1}) in pre-fractionated, trypsin-digested serum in a reproducible manner. As an example, we targeted HSP90α, a protein that is upregulated in various cancers and is thus pursued as a target for early diagnosis, prognosis, and anticancer therapy.[22–24] It plays a crucial role in protein folding and assists in removal of misfolded proteins. In this study, we compared the concentration of HSP90α in 43 sera from healthy subjects measured by SRM, PRM and a commercially available ELISA with respect to comparability, repeatability, and sensitivity.

2. Experimental Section

2.1. Samples

Forty-three serum samples were obtained from the Department of Gynecology (UMCG). All newly referred women were routinely asked to give written informed consent for collection and storage of pretreatment and follow-up serum samples in a serum bank for future research. Relevant data and follow-up results were retrieved and transferred to an anonymous, password-protected database. Identity was protected by study-specific, unique codes and the true identity is only known to two dedicated data managers. According to Dutch regulations, these precautions mean that no further institutional review board approval is needed (http://www.federa.org). The serum samples used for this study were from women referred to the UMCG for an abnormal cytological analysis but who did not show any signs of developing cervical cancer upon follow-up examination. Glass tubes (Becton Dickinson, #367953), with a separation gel and micronized silica to accelerate clotting, were used for blood collection. Serum was prepared by letting freshly collected blood coagulate at room temperature at least for 2 h (till 8 h) followed by centrifugation at room temperature for 10 min at 3000 rpm. Serum samples were stored at −80 °C in aliquots until analysis.

2.2. Prefractionation by SCX Chromatography

Forty-three serum samples from healthy subjects (Supporting Information Table S1) were analyzed and a sample of pooled serum from a separate set of healthy volunteers containing approximately 100 ng mL^{-1} HSP90α was used as quality control (QC1). Seven microliters from each serum sample was diluted 47 times in 0.01% RapiGest SF (Waters, Milford, MA) in 50 mM ammonium bicarbonate pH 7.8, reduced using 15 mM DTT, alkylated with 15 mM iodoacetamide (IA), and subsequently digested by adding 30 μL trypsin (100 μg mL^{-1} 3 mM Tris-HCl pH 8.8) (Gold, MS Grade, Promega, Madison, WI) at 37 °C overnight. The enzymatic reaction was stopped by adding 50% FA in water to reach a final concentration of 0.5–1.0% FA. Digested sera were spiked with 40 fmol of two SIL (stable isotope-labeled) proteotypic peptides YIDQEELNK ($^{13}C_6^{15}N_2$) and DQVANSAFVER ($^{13}C_6^{15}N_4$) (Thermo Fisher Scientific, Bremen, Germany; purity of >97% as stated by the manufacturer (Ultimate grade)). Subsequently, the digested samples were desalted using a macroporous reversed phase mRP-C18 column (Agilent, Palo Alto, California, USA; 4.6 mm × 50 mm) at a flow rate of 750 μL min^{-1} according to Boichenko et al.[25] and offline fractionated on a Luna 5 μm, 150 × 2 mm SCX column (Phenomenex, Torrance, CA) under the following conditions: buffer A (14 mM KH$_2$PO$_4$, 24 mM H$_3$PO$_4$, pH 2.5, adjusted with 37% (w/w) HCl) in 25% (v/v) acetonitrile (HPLC grade; Biosolve, Valkenswaard, the Netherlands) in Milli-Q water; buffer B (buffer A containing 350 mM KCl); linear gradient from 100% buffer A to 40% buffer B in 40 min, followed by a wash with 100% buffer B until 45 min at a flow rate of 200 μL min^{-1} and equilibration of the column in buffer A for 17 min. All chemicals used for SCX fractionation were purchased from Sigma–Aldrich (St Louis, MO). Fifty microliter fractions (180 fractions in total for each serum sample) were collected in 384-well plates (VWR, Amsterdam, the Netherlands) and sealed with an adhesive aluminum foil (VWR, Amsterdam, the Netherlands). Fractions were dried down in SpeedVac concentrator (RVT4104, Scientific Savant, San Jose, CA) and subsequently stored at −20 °C until further analysis. Samples were reconstituted in 0.1% FA prior SRM and PRM measurements. **Figure 1** shows a general flowchart of how the study was performed.

2.3. SRM

SRM for quantitative measurements of HSP90α in the 43 SCX-fractionated serum digests was performed targeting the two proteotypic peptides YIDQEELNK and DQVANSAFVER. The peptides were selected after analyzing a tryptic digest of recombinant HSP90α (Genway Biotech Inc, San Diego, CA) by LC–MS/MS, since they generated the most intense fragment ions. The shotgun MS proteomics data have been deposited to the ProteomeXchange Consortium via the PRIDE[26] partner repository with the dataset identifier PXD007601 and
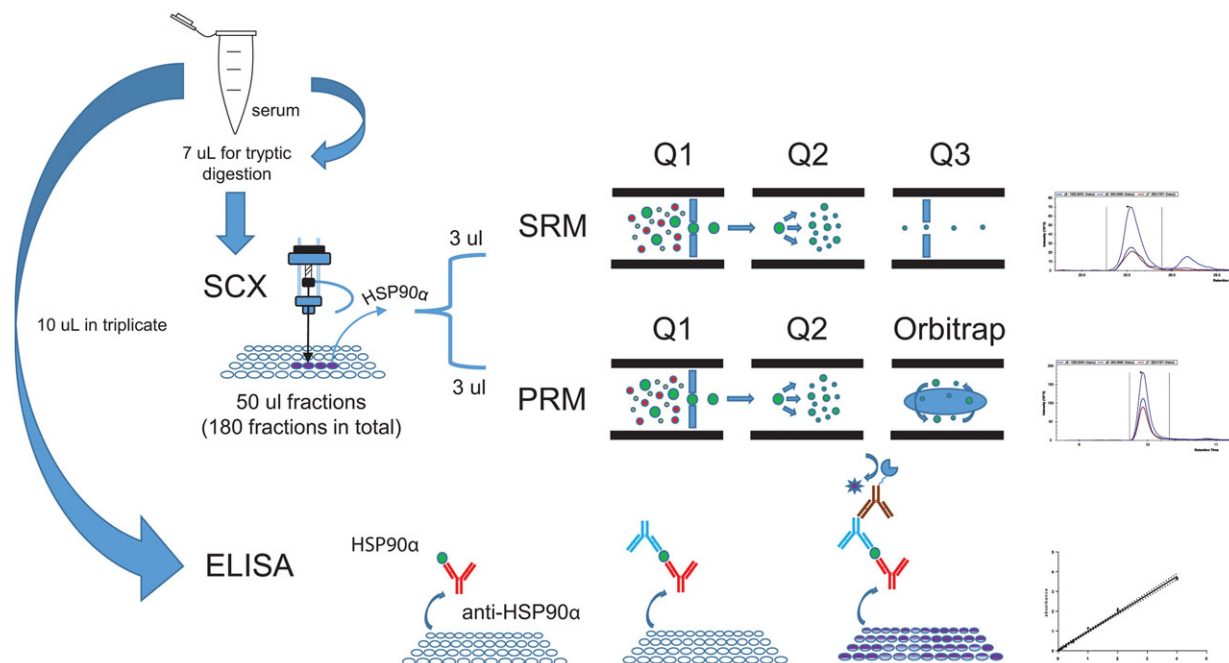
ADVANCED
SCIENCE NEWS
www.advancedsciencenews.com

Proteomics
Clinical Applications
www.clinical.proteomics-journal.com

Figure 1. Flowchart of experimental design.

https://doi.org/10.6019/PXD007601. Peptides containing potential missed cleavage sites, methionine, cysteine or ragged ends KK, KR, and RR were excluded. An online BLAST analysis (Program: NCBI BLASTP 2.2.29, database: UniProtKB database, January 3, 2014) showed that YIDQEELNK can be used to quantify HSP90α (P07900) and HSP90β (P08238) while DQVANSAFVER is specific for HSP90α only (85.8% sequence homology between HSP90α and HSP90β). The possibility of detection of HSP90β is fairly small, since this protein is present at much lower levels in serum levels ($\approx$1–2 ng mL^{-1})[27,28] than HSP90α. SCX-fractionated peptides were separated using a nanoACQUITY LC system equipped with an RP analytical BEH300 C18, 300 Å, 1.7 μm, 75 μm $\times$ 200 mm column. Samples were desalted at a flow rate of 8 μL min^{-1} with a C18 trap column, 5 μm, 100 Å, 180 μm $\times$ 20 mm for 5 min using 0.1% formic acid (FA) in water prior separation. Separation was performed on the above-mentioned analytical column at a flow rate of 300 nL min^{-1} with 0.1% aqueous FA (mobile phase A) and 0.1% FA/ACN (mobile phase B) as solvents with a linear gradient from 1.5% B at 0 min to 40% B at 30 min. The column was washed with 80% B for 4.9 min and equilibrated with 1.5% B for 24.9 min. All LC solvents were UHPLC grade and purchased from Biosolve (Valkenswaard, the Netherlands). The nanoACQUITY LC system was connected to a Xevo TQ-S (Waters Corp., Milford, MA) triple quadrupole mass spectrometer in positive ESI mode. SRM signals were recorded for all samples in a single measurement for the doubly charged peptide precursor ions YIDQEELNK (m/z 580.29 for the $^{13}C_6$$^{15}N_2$ labeled peptide) and DQVANSAFVER (m/z 623.31 for the $^{13}C_6$$^{15}N_4$ labeled peptide). The following parameters were set using a nanoflow Z-spray ion source: capillary voltage 3000 V, nebulizer gas (nitrogen) 0.15 bar, collision gas flow 0.15 mL min^{-1} (argon), source temperature 70 °C, LM/HM (low mass/high mass) quad 1 resolution 3.0/15.20, LM/HM quad

2 resolution 2.90/14.80, ion energy 0.9, and cycle time was set to automatic operation. The selected transitions for YIDQEELNK and DQVANSAFVER are shown in **Table 1**. The indicated collision energy varied from 15–18 and 17–19 V depending on the fragment ion, respectively. The SRM signals were integrated using Skyline software (version 3.5.0.9321) tool[29] and HSP90α concentration was calculated by using the peak area ratio of endogenous and SIL peptide.

The two peptides were found in six (on average) SCX fractions. These six fractions were pooled to obtain a QC2 sample. A serial dilution of five SIL peptide concentrations (calibrants) between 0–30 ng mL^{-1} (i.e. 0, 0.3, 1.2, 3.0, 6.0, and 30.0 ng mL^{-1}) was prepared in the QC2 sample and in its pure condition (dissolved in just 0.1% aqueous FA). Three microliters of each concentration was injected onto the nano-LC–MS. Subsequently, regression analysis was performed by plotting the concentration versus total peak area (of all related y-transitions) of each SIL peptide. The proteomics data (.raw and .mzML files) and the transition list (.csv file) were deposited in the Peptide Atlas SRM Experiment Library assigned with identifier PASS01047 (http://www.peptideatlas.org/PASS/PASS01047).

To determine the variability (in CV%) of the transitions (endogenous and SIL) of YIDQEELNK and DQVANSAFVER for all 43 sera measured, the percent contribution of each transition was calculated by the ratio of its peak area to the total peak area from all transitions for each serum sample. Considering that the intensities of the observed transitions differ considerably, we also calculated weighted CV. The weighted CV (in weighted%) for each transition was calculated by multiplying the CV% with the averaged peak area ratio transition/total transition of the 43 samples. Additionally, the statistical significance (unpaired t-test) was determined of the weighted CVs between YIDQEELNK and DQVANSAFVER (endogenous and SIL) for both SRM and PRM.

Table 1. Selected transitions for YIDQEELNK (y5, y6, and y7) and DQVANSAFVER (y7, y8, and y9) with their corresponding fragment masses that were used to perform quantitative LC–MS/MS assays in the SRM and PRM mode. Both CV and weighted CV (see text for discussion) were calculated from 43 SCX-fractionated serum samples. Significantly, more variation (weighted CV) was observed for endogenous DQVANSAFVER than for YIDQEELNK when measured by SRM. PRM measurements did not show such significant differences. The SIL peptides showed a similar effect, although to a lesser extent because on average five times more SIL peptide was applied than the measured endogenous peptide (one outlier by PRM (sample no. 2, see Supporting Information Figure S3) was observed and this sample was removed from CV analysis only).

Peptide	y5	y6	y7
YIDQEELNK (*m/z* 576.28, +2)	632.33	760.38	875.41
CV%/weighted CV%	SRM: 31.8/2.5	SRM: 47.7/2.6	SRM: 3.9/3.4
	PRM: 13.3/0.7	PRM: 9.9/0.7	PRM: 1.1/1.0
YIDQEELNK (SIL) (*m/z* 580.29, +2)	640.34	768.40	883.43
CV%/weighted CV%	SRM: 21.4/1.3	SRM: 26.2/1.0	SRM: 2.3/2.1
	PRM: 5.4/0.3	PRM: 6.7/0.4	PRM: 0.6/0.5

Peptide	y7	y8	y9
DQVANSAFVER (*m/z* 618.30, +2)	822.41	893.45	992.52
CV%/weighted CV%	SRM: 26.9/5.4	SRM: 15.0/8.0	SRM: 22.3/6.0
	PRM: 3.8/0.9	PRM: 2.5/1.2	PRM: 2.9/0.8
DQVANSAFVER (SIL) (*m/z* 623.31, +2)	832.42	903.46	1002.52
CV%/weighted CV%	SRM: 10.5/2.2	SRM: 5.8/3.1	SRM: 6.0/1.4
	PRM: 1.9/0.4	PRM: 1.2/0.6	PRM: 1.6/0.4

2.4. PRM

The identical 43 SCX-fractionated serum digests and same serial dilutions as described in the previous section were measured by PRM based on a single measurement and analyzed in Skyline. These measurements were carried out on a nano-LC system (Ultimate 3000 RSLCnano, Thermo Fisher Scientific, Germering, Germany) online coupled to an Orbitrap Fusion mass spectrometer (Thermo Fisher Scientific, San Jose, CA, US). Samples were loaded onto a trap column (PepMap C18, 300 μm ID × 5 mm length, 5 μm particle size, 100 Å pore size; Thermo Fisher Scientific), washed and desalted for 5 min using 0.1% TFA/water as loading solvent. Next, the trap column was switched in-line with the analytical column (PepMap C18, 75 μm id × 250 mm, 2 μm particle and 100 Å pore size, Thermo Fisher Scientific). Peptides were eluted with the following binary gradient starting with 12% solvent B for 4 min and then from 12 to 25% solvent B in 14.7 min, where solvent A consisted of 0.1% FA in water, and solvent B consisted of 80% acetonitrile and 0.08% FA in water. The column flow rate was set to 250 nL min^{-1} and the oven temperature to 40 °C. All LC solvents were from identical UHPLC grade as mentioned above in the previous section. For ESI, nano ESI emitters (New Objective, Woburn, MA) were used and a spray voltage of 1.8 kV was applied. For PRM of the doubly charged precursor ions of YIDQEELNK and DQVANSAVER (endogenous and SIL), we used the targeted MS/MS mode set up as follows: isolation width of 1.4 Da, HCD fragmentation at a normalized collision energy of 24%, ion injection time of 502 ms (by setting the AGC target to 500 000 ions), Orbitrap resolution of 240 000. Selection of precursor ions was time scheduled (0–5.8 min for YIDQEELNK; 5.8–20 min for DQVANSAFVER) and each duty cycle consisted of two targeted MS/MS scans (endogenous and SIL form of a peptide) yielding a scan rate of approximately 0.9 Hz. Fluoranthene (202.0777 Da) was infused as lock

mass (Easy IC option active). The MS proteomics data have been deposited to the ProteomeXchange Consortium via the PRIDE[26] partner repository with the dataset identifier PXD006618 and https://doi.org/10.6019/PXD006618.

The variabilities (CV and weighted CV) of each fragment ion were calculated as described above for SRM. To investigate the effect of MS/MS resolution independently from different instrumental parameters, we set up a PRM method where MS/MS detection was conducted in the linear ion trap (resolution approximately 0.35 Da FWHM) of the Orbitrap Fusion MS. The value of a high-resolution mass spectrometer (PRM) in contrast to a triple-quad instrument (SRM) was demonstrated by comparing the presence of co-eluting peaks and MS2 spectra with identical samples (four SCX fractions) measured in PRM and by PRM at quadrupole ion trap resolution (IT-PRM) of the Orbitrap instrument under identical conditions. The IT-PRM method was set up in such a manner that MS/MS spectra were acquired in the ion trap (normal scan rate, AGC target of 100 000 ions, and maximum injection time of 500 ms). All other parameters were identical to the common PRM method described above. To exclude that differences between SRM and PRM are an effect of different experimental setup (such as type of column, gradient, and run time) four fractions of three different SCX-fractionated serum digests with relative high co-eluting peaks which were observed by SRM were also measured by IT-PRM. To gain insight in the effects of co-elution, peak ratios (between peak areas) were calculated between transitions of the endogenous peptides YIDQEELNK and DQVANSAFVER at the apex, half-height, and one-quarter-height on the right side of the mass spectral peak and corresponding SIL peptides in pure condition (0.1% aqueous FA). The weighted CVs were calculated as described above for each transition at each peak height and evaluated. It was assumed that intensities and ratios were similar if interferences were not present.

ADVANCED
SCIENCE NEWS
www.advancedsciencenews.com

Proteomics
Clinical Applications
www.clinical.proteomics-journal.com

2.5. Data Analysis (LOD/LOQ, Repeatability, Reproducibility, and Stability)

Linearity, LOD, and LOQ of the HSP90α-derived peptides were calculated based on the slope (S) and the residual standard deviation of the slope (σ) from linear regression analysis according to ICH guidelines (http://www.ich.org) for single measurements. The LOD was defined as $3.3 \times \sigma/S$ and the LOQ as $10 \times \sigma/S$. Correlations were plotted to determine the relationship between both endogenous HSP90 peptides and linear regression coefficients were calculated.

To evaluate the repeatability, three technical replicates (three SRM or PRM measurements of an SCX-fractionated QC1 sample) were measured over a short time period (<4 days; kept at 4 °C), and CVs in percentages were calculated. Additionally, for stability testing the SCX-fractionated QC1 sample was repeatedly measured over a longer period with long-term intervals (ranging from 4 days to 6 months) and were kept at 4 °C during storage) by SRM and PRM. CVs of HSP90α concentrations were calculated for both YIDQEELNK and DQVANSAFVER. To determine the matrix effect on the two SIL peptides, a regression analysis was performed of pure (dissolved in 0.1% aqueous FA) and matrix-spiked (spiked into background of SCX fractions) samples over a range of 0–30 ng mL^{-1} (described above in the section: "SRM") measured by SRM and PRM. From these calibration curves the slopes were compared between both matrix-spiked and pure SIL peptides. We calculated the ratio (expressed in percentages) of the mean peak areas of calibrants related to matrix-spiked and pure SIL peptides. Statistical differences were calculated and a probability lower than 0.05 was considered to be significant.

2.6. ELISA-Based Quantification

HSP90α was quantified in the identical set of 43 sera including the QC1 sample with a commercial ELISA (Enzo Life Science, ADI-EKS-895). This assay has been described in several publications.[30–33] Briefly, 100 μL of diluted serum (1:10 in Sample Diluent buffer) was incubated for 1 h at room temperature in the microtiter plate precoated with anti-HSP90α antibody. Subsequently, a 400× diluted HSP90α monoclonal antibody conjugated to HRP in HRP diluent was added followed by stabilized tetramethylbenzidine substrate solution. The reaction was stopped by adding 100 μL of acidic stop solution provided by the manufacturer. The HSP90α standard (part no. 80–1564, Enzo Life Science, ADI-EKS-895) with seven dilutions (i.e. 0.0625, 0.125, 0.250, 0.500, 1.000, 2.000, and 4.000 ng mL^{-1} including a zero standard) was used for calibration. The absorbance for individual samples and the serial dilutions (two microtiter plates in total) were measured on a Multiscan Ascent microtiter plate reader (Thermo Electron, Marietta, Ohio, USA) at 450 nm. To determine the repeatability, each serum sample was measured in triplicate on the microtiter plate to calculate intra-microtiter plate variation (mean CV%). Four samples were measured on different ELISA plates to calculate inter-microtiter plate variation (mean CV%). Both LOD and LOQ were determined by a linear regression analysis in analogy to the SRM and PRM measurements. HSP90α levels obtained in SRM and PRM mode were compared to ELISA measurements by correlation plots. Bland–Altman plots for the ELISA to SRM/PRM method comparison were constructed showing 95% limits of agreement. Methods were considered to be in agreement if the chosen mean bias interval was within ± 5%. The significance of these method comparisons was determined by the Welch t-test.

2.7. Comparability of SIL Peptides and Immunoassay Standard

To determine the comparability of the SRM and PRM based on the SIL peptides and the immunoassay recombinant HSP90α standard (1 μg mL^{-1}; calibration standard provided with the ELISA kit), an amount of 4 ng of the HSP90 SIL peptides was mixed with 2 ng of the immunoassay standard and reduced (5.1 mM DTT), alkylated (15.1 mM IA), and trypsin (50 ng) digested at 37 °C overnight. The sample which corresponded to 56.7 pg on column (3 μL of injection volume) was measured in triplicate by SRM and PRM as described before. Subsequently the ratios between the endogenous peptides of the HSP90α standard and SIL peptides were used to determine the HSP90α concentration. Additionally, to assess the purity of the protein standard a data dependent acquisition was used. For nano-LC separation (also 3 μL of corresponding sample), a linear gradient from 4 to 38% solvent B in 90 min was used and followed by a shotgun method with Orbitrap MS1 acquisition from m/z 400–1600 at 120 000 resolution (AGC = 40 000 ions) followed by ion trap CID MS/MS spectra (30% normalized collision energy, AGC = 10 000 ions, and maximum injection time of 40 ms) for at most 3 s ('top-speed' type data-dependent acquisition method). Peptides were identified and assigned to proteins by exporting features, for which MS/MS spectra were recorded, using the ProteoWizard software (version 3.0.9248; http://proteowizard.sourceforge.net). Resulting .mgf file was submitted to Mascot (version 2.3.02, Matrix Science, London, UK) and applied to the human database (UniProtKB/Swiss-Prot, version 151112, 20194 entries) for protein identifications. The following parameters were used: fragment ion mass tolerance of 0.50 Da, parent ion mass tolerance of 10 ppm, and maximum number of missed cleavages of two. In the Mascot search engine oxidation of methionine was specified as a variable modification while carbamidomethylation of cysteine was set as a fixed modification. Scaffold software (version 4.7.5, Proteome Software Inc., Portland, OR) was used to compute protein grouping, peptide probabilities, and protein probabilities.[34] Peptides identified with Mascot ions sore >25 were considered to be true identifications. The MS proteomics data have been deposited to the ProteomeXchange Consortium via the PRIDE[26] partner repository with the dataset identifier PXD006615 https://doi.org/10.6019/PXD006615.

2.8. LOD/LOQ Comparison of PRM with ELISA

LOD/LOQ obtained by HSP90α ELISA were compared with PRM only (not measured by SRM due to too low sensitivity). For this purpose, serial dilutions of SIL peptides were prepared in the pooled fraction of the SCX-fractionated QC1 sample (as described above in the section: "ELISA-based quantification") containing comparable concentrations of the HSP90α calibrants

ADVANCED
SCIENCE NEWS

www.advancedsciencenews.com

Proteomics
Clinical Applications

www.clinical.proteomics-journal.com

used for ELISA. The LOD and LOQ were calculated using regression analysis as described above in the section: "Data analysis".

3. Results

We combined fractionation of peptides by SCX chromatography of trypsin-digested serum with LC–MS in the SRM or the PRM mode to quantify HSP90α and compared the results with a commercially available HSP90α ELISA.

3.1. Linearity, LOD, and LOQ of SRM, PRM, and ELISA by Linear Regression Analysis

An overview of the calculated LODs and LOQs for both SRM and PRM assays (concentration range 0–30 ng mL^{-1}), and for the ELISA, for which a linear regression analysis was performed as recommended by manufacturer (concentration range 0–4 ng mL^{-1}), is shown in **Table 2**. In addition, from an independently prepared serial dilution (comparable to the ELISA range from 0–4 ng mL^{-1}, according to the manufacturer) measured by PRM, an R^2 of 0.986 and 0.989 was obtained for YIDQEELNK between ELISA and DQVANSAFVER between ELISA, respectively. In the PRM measurements and from regression analysis, the LOD for both YIDQEELNK and DQVANSAFVER was found to be 0.5 ng mL^{-1}. An LOQ of 1.6 and 1.5 ng mL^{-1} was calculated for YIDQEELNK and DQVANSAFVER, respectively. These values are significantly lower than those listed in Table 2 and are on a par with those obtained by ELISA. It can be seen from Table 2 that in the SRM mode the LOD and LOQ values for both peptides are considerably larger (by a factor of about 6) than in the PRM mode, attesting to the superiority of the PRM method.

Table 2. Calculated LOD and LOQ levels in ng mL^{-1} for HSP90α in the pooled fraction of the SCX-fractionated QC1 sample based on SIL peptides YIDQEELNK and DQVANSAFVER for SRM, PRM, and for comparable HSP90α ELISA measurements.

SRM		
Peptide	LOD (ng mL^{-1})	LOQ (ng mL^{-1})
YIDQEELNK	5.6	17.4
DQVANSAFVER	6.7	20.4
PRM		
Peptide	LOD (ng mL^{-1})	LOQ (ng mL^{-1})
YIDQEELNK	1.0 (0.5)[a]	2.9 (1.6)[a]
DQVANSAFVER	1.3 (0.5)[a]	3.8 (1.5)[a]
ELISA		
Cat No. ADI-EKS-895, Enzo Life Science	LOD (ng mL^{-1})	LOQ (ng mL^{-1})
HSP90α specific mouse monoclonal antibody	0.4	1.2

[a]Calculated if the same standard dilutions were used as described by the manufacturer of the ELISA.

Calibration curves for the two HSP90α SIL peptides spiked into the pooled fraction of the SCX-fractionated QC1 sample as well as for pure standards based on five serial dilutions (i.e. 0, 0.3, 1.2, 3.0, 6.0, and 30.0 ng mL^{-1}) are shown in Supporting Information Figure S1. High correlations between results of matrix-spiked and pure conditions were obtained in PRM (>0.990). To determine effects due to matrix, the mean ratios were calculated between the peak areas for the matrix-spiked and pure conditions of all calibrants (0.3–30 ng mL^{-1}) based on the calibration curves as seen in Supporting Information Figure S1. SRM gave mean ratios of 252.3 and 295.9% for YIDQEELNK and DQVANSAFVER, respectively. Similar ratios were obtained for PRM for YIDQEELNK and DQVANSAFVER with 217.3 and 241.4%, respectively. Thus, peptides spiked into matrix consistently gave a stronger response compared to the pure peptide dissolved in 0.1% aqueous FA especially at low ng mL^{-1} concentrations. This may be due to low adsorption as a result of other (sacrificial) matrix peptides which bind to the surface of the vial, as also observed for oligonucleotides.[35] Linearity was better for peptides spiked into matrix compared to those spiked into 0.1% aqueous FA for SRM and PRM measurements.

3.2. Comparison of the Repeatability and Stability of SRM, PRM, and ELISA Assay

The repeatability of PRM was significantly better than for SRM for both peptides YIDQEELNK (CV of 1.1% for PRM versus 8.4% for SRM) and DQVANSAFVER (CV of 1.8% for PRM versus 11.8% for SRM, see Supporting Information Table S2). Repeatability for PRM was also superior compared to the commercial ELISA assay (intra-microtiter plate CV of 4.2%; inter-microtiter plate mean CV of 7.5%, see Supporting Information Table S2).

The stability experiments showed CVs of 15.6% for YIDQEELNK and 17.7% for DQVANSAFVER from repeated measurements by SRM and 4.5 and 8.9% for PRM, respectively.

3.3. Quantification of HSP90α by SRM, PRM, and ELISA in Serum

Supporting Information Table S1 shows serum HSP90α levels measured based on the proteotypic peptides YIDQEELNK relating to the α and β isoforms and DQVANSAFVER relating to the α isoform, by SRM and PRM in comparison to ELISA. Both SRM and PRM assays had adequate sensitivity to quantify HSP90α in all trypsin-digested, SCX-fractionated serum samples. The mean concentration of HSP90α across all sera measured by SRM was 73.4 $\pm$ 32.8 ng mL^{-1} based on the YIDQEELNK peptide, while the DQVANSAFVER peptide gave a significantly (unpaired t-test, $p = 0.001$) higher concentration of 108.4 $\pm$ 60.7 ng mL^{-1}, due to a higher variance (see **Figure 2**A; more examples are shown in Supporting Information Figure S2 in Supporting Information). The mean concentration of HSP90α in the same set of samples based on PRM measurements of the peptides YIDQEELNK and DQVANSAFVER was 118.8 $\pm$ 66.7 ng mL^{-1} and 128.1 ng mL^{-1} $\pm$ 72.7 ng mL^{-1}, respectively, and these concentrations were not different (unpaired t-test, $p = 0.539$). Possible interference of

**ADVANCED
SCIENCE NEWS**
www.advancedsciencenews.com

**Proteomics
Clinical Applications**
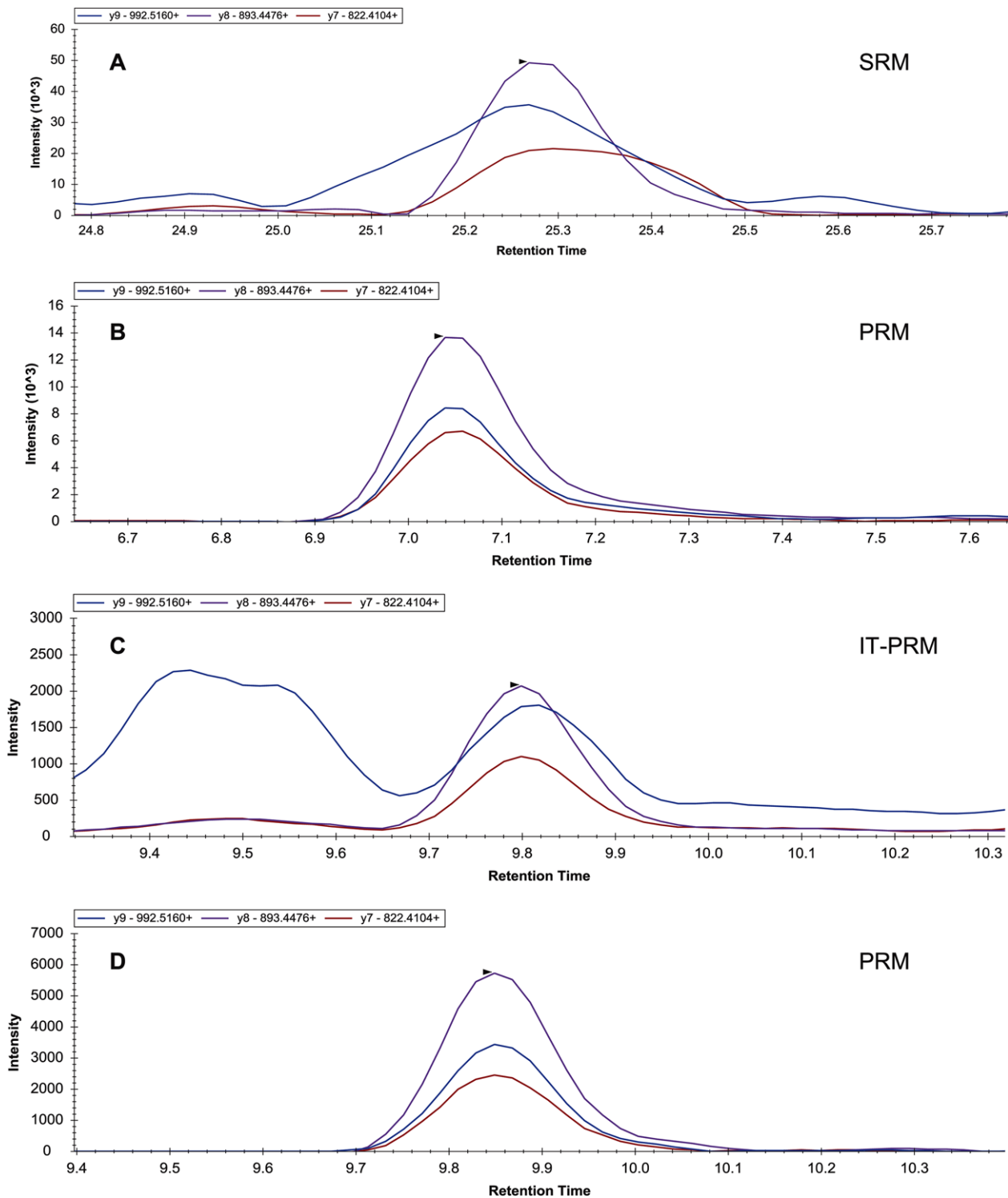www.clinical.proteomics-journal.com

Figure 2. SRM, PRM, and IT-PRM chromatograms of an identical SCX-fractionated serum sample (sample no. 28, see Supporting Information Table S1) as observed in Skyline. An example of co-eluting peaks by means of misaligned transitions (y7, y8, and y9) for DQVANSAFVER was observed in SRM (A) and IT-PRM (C). For comparison, the identical sample was measured by PRM simultaneously with SRM and IT-PRM measurements (B and D, respectively). More examples of these probable interfering co-eluting peaks are shown in Supporting Information Figure S2 and S7.
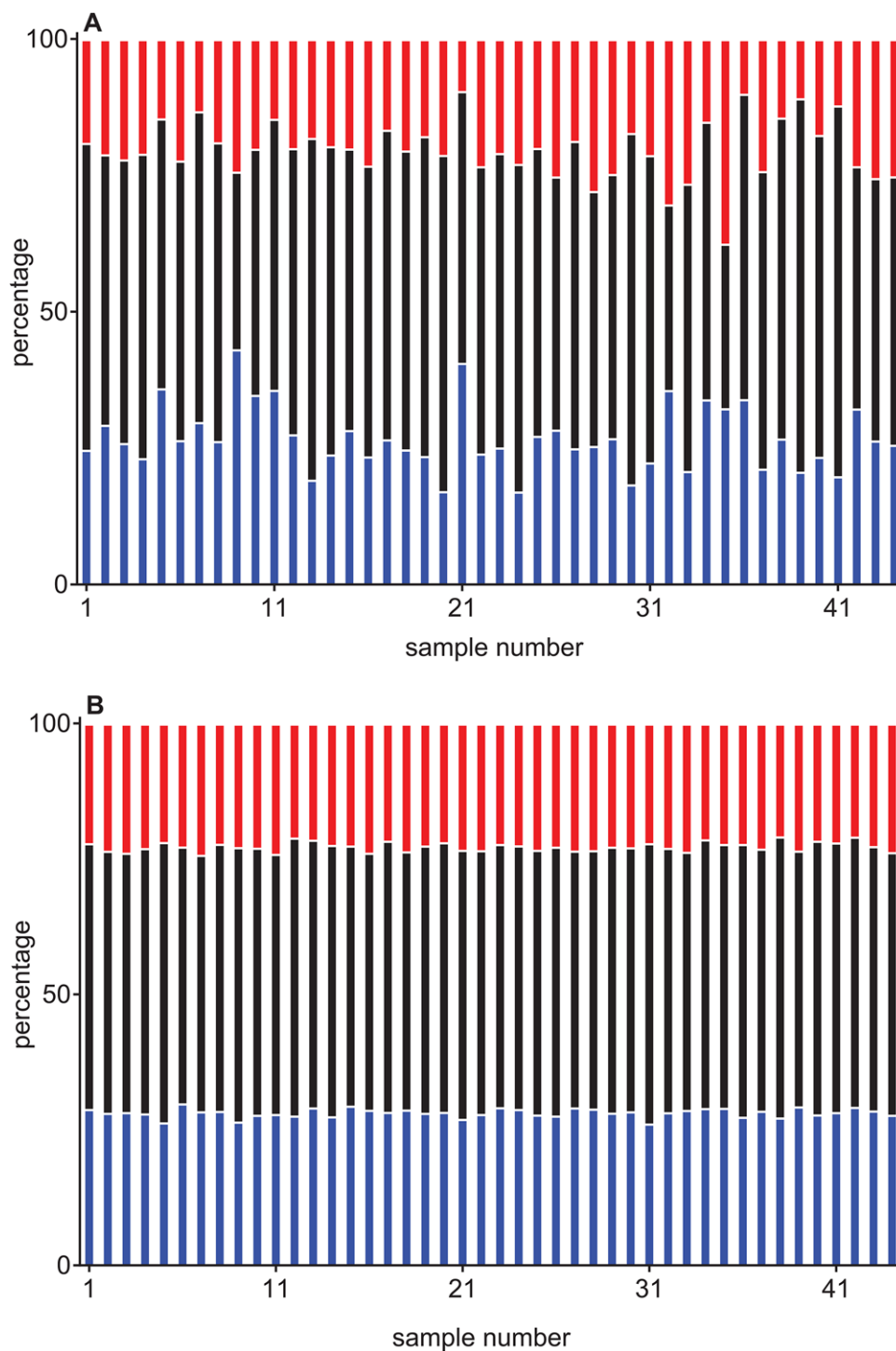
ADVANCED
SCIENCE NEWS
www.advancedsciencenews.com

Proteomics
Clinical Applications
www.Clinical.proteomics-journal.com

Figure 3. Representation of the variability in the transitions of the HSP90α proteotypic peptide DQVANSAFVER measured by SRM (A) and PRM (B). Bars represent normalized peak areas (% of total) of the transitions y7 (red), y8 (black), and y9 (blue) in 43 SCX-fractionated serum samples from healthy subjects. Sample number 44 corresponds to 1 fmol of the pure (0.1% aqueous FA) SIL peptide. See Supporting Information Figure S3 for the corresponding results for YIDQEELNK.

co-eluting compounds was not observed in PRM due to the higher mass resolution (see Figure 2B or 1D and Supporting Information Figure S2). The CVs for the most intensive DQVANSAFVER-related transition y8 were 15.0% and 5.8% in SRM and 2.5% and 1.2% in PRM for the endogenous and the SIL peptides, respectively (Table 1; **Figure 3**). Comparison of the weighted CVs for the y-ions of YIDQEELNK with y-ions of DQVANSAFVER showed that these CVs were significantly different for SRM but not for PRM indicating interference in the SRM assay. For both SRM and PRM the SIL peptides showed better weighted CVs compared to the endogenous peptides, but the concentration of the SIL peptides was higher (on average five times).

The correlation between HSP90α concentrations based on SRM measurements of YIDQEELNK and DQVANSAFVER was poor with an R^2 of 0.642 (Supporting Information Figure S4A; Supporting Information Table S3) and significantly worse compared to PRM ($R^2 = 0.894$). Correlations above 0.7 were considered as good.[36] To compare the SRM and PRM measurements with an established assay, the same serum samples were measured with a commercially available HSP90α ELISA as illustrated in Supporting Information Figure S5, giving an average concentration of 113.7 $\pm$ 60.1 ng mL^{-1}. This was in excellent agreement (unpaired t-test, $p = 0.465$) with the PRM measurements for both peptides (average 123.9 $\pm$ 69.6 ng mL^{-1}). Comparison of PRM with ELISA showed an R^2 of 0.878 and 0.811 for YIDQEELNK and DQVANSAFVER, respectively (Supporting Information Figure S4E and F; Supporting Information Table S3). Correlation was not significantly different for YIDQEELNK ($p = 0.709$) and DQVANSAFVER ($p = 0.295$) as determined by the Welch t-test. Correlation of SRM and ELISA data reached R^2 values of 0.764 and 0.652 for YIDQEELNK and DQVANSAFVER peptides, respectively (Supporting Information Figure S4C and D; Supporting Information Table S3). Measured concentrations of HSP90α were significantly different for the SRM assay based on YIDQEELNK ($p < 0.001$) and the ELISA results but not for SRM based on DQVANSAFVER ($p = 0.686$) although significantly more variation was observed for DQVANSAFVER than for YIDQEELNK (Table 1 and Figure 2 and Supporting Information Figure S3). Comparison of the measured concentrations by SRM and PRM with the ELISA in a Bland–Altman plot with a $\pm$ 95% confidence interval showed a bias of –41.0% for the YIDQEELNK endogenous peptide measured in SRM (Supporting Information Figure S6), while PRM had a bias of 3.9 %. The bias for DQVANSAFVER was –5.7 and 11.1% by SRM and PRM, respectively. The kind and degree of interference of unknown components can vary from sample to sample and this causes SRM signals to display a much larger spread than PRM signals because these unknown components have less chance to be included in the PRM experiments, see Figure **3**.

3.4. Comparability of SIL Proteotypic Peptides with HSP90α as Calibration Standard

One major difference between MS-based methods and the ELISA assay is that the first uses stable isotope labeled, synthetic, and proteotypic peptides as standards while the latter uses HSP90α

protein. In order to make a link between these two principles of assay calibration, we mixed 4 ng of our SIL peptides with 2 ng of the ELISA standard as described in the section: "Experimental Section" and measured the HSP90α concentration by SRM and PRM, respectively. In this way, the final concentration of the ELISA standard is 1.0 μg mL^{-1}. SRM and PRM measurements based on YIDQEELNK gave 1.4 and 1.1 μg mL^{-1} HSP90α, respectively. Both SRM and PRM measurements based on DQVANSAFVER gave a significantly lower concentration of 0.36 μg mL^{-1} HSP90α. To gain a better insight into this unexpected discrepancy, we evaluated the purity of the HSP90α ELISA standard by shotgun proteomics using a data-dependent acquisition approach. A database search resulted in 32 (Supporting Information Table S4) identified proteins of which the top five hits (based on number of exclusive unique peptide counts) were related to high-abundant proteins (e.g. serum albumin, various types of keratin I and II) while HSP90α was ranked halfway of the list. The results showed further that identification of HSP90α was based on only 2% sequence coverage related to one peptide that did not correspond to the two selected proteotypic peptides used for this study. The protein complexity of the ELISA standard used in the ELISA could well explain the discrepancy observed above between ELISA and MS based techniques (SRM and PRM). Thus, these results show that while the HSP90α ELISA standard can be ideal for immunoassays, it is not very easy to use in MS based analyses because the HSP90α ELISA standard contains other proteins.

3.5. High-Resolution PRM and PRM at Quadrupole Mass Resolution (IT-PRM)

To rule out the possibility that the discrepancy observed between SRM and PRM is due to instrument effects, we measured four fractions of three different SCX-fractionated serum digests (sample no. 9, 28, and 32; Supporting Information Table S1) by SRM, IT-PRM (PRM at quadrupole ion trap resolution), and PRM (high-resolution) (Figure 2 and Supporting Information Figure S7). Co-eluting peaks seen in SRM were also observed in IT-PRM; while in PRM, no such observation was observed for identical samples by applying the appropriate resolution settings during data analysis. The variation of transitions related to endogenous and the SIL peptides YIDQEELNK and DQVANSAFVER measured by IT-PRM and PRM at three points (apex, half-height, and one-quarter-height) of the peak is illustrated in Supporting Information Figure S8. For PRM, the intensities of each transition extracted from the three measured points of the endogenous peptides showed little aberration (weighted CV of $\approx$3% for both YIDQEELNK and DQVANSAFVER, Supporting Information Table S5), while variation for IT-PRM was considerably larger (highest weighted CV of 33.1% (y7-ion) for YIDQEELNK; highest weighted CV of 9.9% (y9-ion) for DQVANSAFVER, Supporting Information Table S5; see for more details Supporting Information Figure S9). Transitions for pure SIL peptides showed almost identical intensities at the three measurement points by IT-PRM and PRM. These results show that the poorer performance of SRM in comparison to PRM is due to the lower resolution of ion analysis rather than instrumental parameters.

**ADVANCED
SCIENCE NEWS**

www.advancedsciencenews.com

**Proteomics
Clinical Applications**

www.clinical.proteomics-journal.com

4. Discussion

We developed a quantitative 2D-LC–MS/MS assay using SRM and PRM technology to measure HSP90α concentrations relating to two proteotypic peptides YIDQEELNK and DQVANSAFVER. The DQVANSAFVER is HSP90α specific, while the peptide YIDQEELNK relates to both HSP90α and β isoforms. However, it is very likely that only the α isoform was measured due to presence of a very low contribution in serum of the β isoform ($\approx$1–2 ng mL^{-1}) as known from literature.[27,28] Both YIDQEELNK and DQVANSAFVER peptides could have posttranslational modifications like phosphorylation considering the presence of serine and tyrosine in their sequence. It is very unlikely that these peptides are phosphorylated according to literature (http://www.uniprot.org). However, some references (http://www.phosphosite.org)[37–39] indicate that phosphorylation site of S505 can be phosphorylated in a few cell lines. By phosphoproteomics of cervical tissue and serum from a healthy volunteer, we could not detect such phosphorylation using TiO$_2$-based phosphopeptide enrichment for both peptides YIDQEELNK and DQVANSAFVER. Therefore, we assume that the contribution of phosphorylation is negligible.

To achieve sufficient sensitivity to detect HSP90α peptides, trypsin-digested sera were fractionated by SCX chromatography. Both HSP90 peptides were highly stable in SCX-fractionated serum and thus very suitable for this comparison. Comparison of the data of high-resolution MS in PRM mode compared to SRM showed significant better performance for PRM with respect to linearity, repeatability, sensitivity, and the almost complete removal in PRM of components which co-elute in SRM. This resulted for PRM in a better LOD and LOQ compared to SRM and an almost identical LOD/LOQ ratio compared to ELISA. PRM results for both endogenous YIDQEELNK and DQVANSAFVER gave comparable levels to ELISA measurements ($p = 0.709$ and 0.295, respectively) and correlated better for both peptides with ELISA data ($R^2 = 0.878$ and 0.811, respectively) than levels obtained by SRM ($R^2 = 0.764$ and 0.652, respectively; Supporting Information Figure S4). SRM results based on YIDQEELNK differed significantly ($p < 0.001$) from the results of a commercial HSP90α ELISA, while those from the other peptide DQVANSAFVER showed no significant difference ($p = 0.686$). This was unexpected because intense co-eluting peaks were observed for DQVANSAFVER but not for YIDQEELNK in SRM mode. From this, it can be concluded that co-eluting peaks do not correlate linearly with the observed differences. PRM showed almost no detectable co-eluting peaks (Figure 3) as was observed in SRM. Altogether PRM for YIDQEELNK- and DQVANSAFVER-derived fragment ions compared to SRM fragment ions resulted in much better weighted CVs as shown in Table 1. Significantly, more variation (weighted CV) was observed for endogenous DQVANSAFVER than for YIDQEELNK when measured by SRM, while PRM measurements did not show significant differences. The SIL peptides showed a similar effect, but to a lesser extent because on average five times more SIL peptide was used than the measured endogenous peptide. It is the variability of interfering (unidentified) components which causes the SRM signals to display a much larger spread than PRM signals, as also exemplified in Figure 3.

PRM is a technique that monitors all product ions within a certain scan range meaning that fragment ion intensities are available for all observed fragments in PRM in contrast to SRM. For this reason, beyond the preselected ions (y5, y6, y7, y8, and y9 for both HSP90 peptides) more transitions can be evaluated. Selecting other transitions than used in this study did not affect the results; for comparison reasons only the transitions used for SRM were analyzed.

To rule out that discrepancies between SRM and PRM that were caused by a variation in experimental conditions (for instance chromatography), four SCX fractions were measured by IT-PRM (to resemble a triple quadrupole instrument as close as possible) and PRM on identical sample material in the same device. It is expected that distribution of the transition intensities should align to each other if no interfering of co-eluting peaks (as demonstrated for the pure SIL peptides) were present. The deviation of the ideal situation became larger for low intensity mass transitions related to both endogenous peptides observed by PRM measurements, while in IT-PRM mode significantly more deviation for all transitions (low and high intense) was noted compared to the pure peptide. This emphasized that SRM and IT-PRM are more susceptible to variation than PRM due to the lower mass resolution of the fragment ion spectra. Differences achieved by PRM were, therefore, not due to different sample handling, ion-generation, or chromatography, but due to the application of high-resolution MS that reduced the number of co-eluting peaks that potentially generate interference. By the application of high-resolution MS, a much better selection of the peptide of interest and its transitions can be made than in a triple quadrupole and possible interferences of neighboring co-eluting peaks can be avoided resulting in better sensitivity and repeatability. Overall, PRM resulted in better analytical performance for the YIDQEELNK and DQVANSAFVER peptides (both endogenous and SIL) compared to SRM.

The accurate determination of the amount of molecules is different for immunoassay and PRM. In immunoassay, mostly a recombinant protein is used that can be accurately measured by a protein assay. In these determinations, it is assumed that a recombinant protein mimics the protein present in a tissue or a biofluid. In SRM and PRM, SIL peptides are synthesized, purified, and an accurate composition of amino acids is determined assuming resemblance with the peptide, which is part of the protein of interest. Therefore, variations in the correct concentration of standards can be expected in these techniques. Bland–Altman plots (Supporting Information Figure S6) were calculated to determine whether the SRM and PRM were in agreement with ELISA results. From this, it was concluded that the YIDQEELNK peptide measured by PRM (and no peptides for SRM) was similar to ELISA measurements based on chosen criteria (within $\pm$ 5% bias interval level). For the peptide DQVANSAFVER measured by PRM, it was not expected that it would fall outside the criteria of 5% (i.e. 11.1%), since it reached in general good results in all conditions as described before in terms of repeatability, low LOD/LOQ, no co-eluting peaks, and good correlation with ELISA. However, as was discussed above (see Table 1), the peptide DQVANSAFVER was found to generally perform slightly less than YIDQEELNK.

**ADVANCED
SCIENCE NEWS**
www.advancedsciencenews.com

**Proteomics
Clinical Applications**
www.clinical.proteomics-journal.com

Comparability experiments in which the HSP90α level of the ELISA standard was determined by SRM and PRM measurements revealed that the discrepancy might be explained by the presence of many other proteins than HSP90α in this HSP90α standard. Likely, the presence of these extra proteins could influence the SRM and PRM measurements if no fractionation is performed.

We demonstrated the high reproducible, robustness, and sensitive PRM assay to determine HSP90α concentrations in SCX-fractionated sera at relative low ng mL^{-1} level. The sensitivity by PRM was in agreement as determined by ELISA data and showed better repeatability. By PRM and SRM, the quality of samples can easily be assessed by an aberrant transition distribution (Figure 3), whereas by ELISA results caused by aberrations in the assay are much more difficult to detect.

If fractionation of biological samples is technically feasible, PRM can be used as an attractive alternative for immunoassay to quantify highly reproducible proteins at the ng mL^{-1} scale in complex protein mixtures including sera without the use of antibodies or comparable binders.

Abbreviations

IT-PRM, parallel reaction monitoring at quadrupole ion trap resolution; SIL, stable isotope-labeled

Supporting Information

Supporting Information is available from the Wiley Online Library or from the author.

Acknowledgements

Conflict of Interest

The authors have declared no conflict of interest.

Keywords

[1] M. S. Bereman, B. MacLean, D. M. Tomazela, D. C. Liebler, M. J. Mac-Coss, *Proteomics* **2012**, *12*, 1134.

[2] H. Keshishian, T. Addona, M. Burgess, E. Kuhn, S. A. Carr, *Mol. Cell. Proteomics* **2007**, *6*, 2212.

[3] K. H. Kim, Y. H. Ahn, E. S. Ji, J. Y. Lee, J. Y. Kim, H. J. An, J. S. Yoo, *Anal. Chim. Acta* **2015**, *882*, 38.

[4] T. Hembrough, S. Thyparambil, W. L. Liao, M. M. Darfler, J. Abdo, K. M. Bengali, P. Taylor, J. Tong, H. Lara-Guerra, T. K. Waddell, M. F. Moran, M. S. Tsao, D. B. Krizman, J. Burrows, *Clin. Proteomics* **2012**, *9*, 5.

[5] T. Shi, D. Su, T. Liu, K. Tang, D. G. Camp, 2nd, W. J. Qian, R. D. Smith, *Proteomics* **2012**, *12*, 1074.

[6] W. Zhi, M. Wang, J. X. She, *Rapid Commun. Mass Spectrom.* **2011**, *25*, 1583.

[7] C. Guzel, N. T. Ursem, L. J. Dekker, P. Derkx, J. Joore, E. van Dijk, G. Ligtvoet, E. A. Steegers, T. M. Luider, *J. Proteome Res.* **2011**, *10*, 3274.

[8] V. Lange, P. Picotti, B. Domon, R. Aebersold, *Mol. Syst. Biol.* **2008**, *4*, 222.

[9] P. Bults, N. C. van de Merbel, R. Bischoff, *Exp. Rev. Proteomics* **2015**, *12*, 355.

[10] J. F. Rusling, C. V. Kumar, J. S. Gutkind, V. Patel, *Analyst* **2010**, *135*, 2496.

[11] P. J. Tighe, R. R. Ryder, I. Todd, L. C. Fairclough, *Proteomics Clin. Appl.* **2015**, *9*, 406.

[12] A. C. Peterson, J. D. Russell, D. J. Bailey, M. S. Westphall, J. J. Coon, *Mol. Cell. Proteomics* **2012**, *11*, 1475.

[13] Y. J. Kim, S. Gallien, V. El-Khoury, P. Goswami, K. Sertamo, M. Schlesser, G. Berchem, B. Domon, *Proteomics* **2015**, *15*, 3116.

[14] G. E. Ronsein, N. Pamir, P. D. von Haller, D. S. Kim, M. N. Oda, G. P. Jarvik, T. Vaisar, J. W. Heinecke, *J. Proteomics* **2015**, *113*, 388.

[15] J. L. Sowers, B. Mirfattah, P. Xu, H. Tang, I. Y. Park, C. Walker, P. Wu, F. Laezza, L. C. Sowers, K. Zhang, *Anal. Chem.* **2015**, *87*, 10006.

[16] Q. Yu, B. Liu, D. Ruan, C. Niu, J. Shen, M. Ni, W. Cong, X. Lu, L. Jin, *Proteomics* **2014**, *14*, 2417.

[17] S. Gallien, S. Peterman, R. Kiyonami, J. Souady, E. Duriez, A. Schoen, B. Domon, *Proteomics* **2012**, *12*, 1122.

[18] Y. J. Kim, S. Gallien, J. van Oostrum, B. Domon, *Proteomics Clin. Appl.* **2013**, *7*, 739.

[19] A. Lesur, B. Domon, *Proteomics* **2015**, *15*, 880.

[20] S. Gallien, S. Y. Kim, B. Domon, *Mol. Cell. Proteomics* **2015**, *14*, 1630.

[21] S. Gallien, A. Bourmaud, S. Y. Kim, B. Domon, *J. Proteomics* **2014**, *100*, 147.

[22] A. Haque, Q. Alam, M. Z. Alam, E. I. Azhar, K. H. Sait, N. Anfinan, G. Mushtaq, M. A. Kamal, M. Rasool, *Curr. Pharm. Des.* **2016**, *22*, 2947.

[23] J. J. Barrott, T. A. Haystead, *FEBS J.* **2013**, *280*, 1381.

[24] D. R. Ciocca, S. K. Calderwood, *Cell Stress Chaperones* **2005**, *10*, 86.

[25] A. P. Boichenko, N. Govorukhina, H. G. Klip, A. G. van der Zee, C. Guzel, T. M. Luider, R. Bischoff, *J. Proteome Res.* **2014**, *13*, 4995.

[26] J. A. Vizcaino, A. Csordas, N. del-Toro, J. A. Dianes, J. Griss, I. Lavidas, G. Mayer, Y. Perez-Riverol, F. Reisinger, T. Ternent, Q. W. Xu, R. Wang, H. Hermjakob, *Nucleic Acids Res.* **2016**, *44*, D447.

[27] B. Rong, C. Zhao, H. Liu, Z. Ming, X. Cai, W. Gao, S. Yang, *Am. J. Cancer Res.* **2016**, *6*, 1460.

[28] B. Rong, X. Cai, H. Liu, T. Fu, W. Gao, C. Zhao, Y. Lin, *Am. J. Transl. Res.* **2016**, *8*, 4147.

[29] B. MacLean, D. M. Tomazela, N. Shulman, M. Chambers, G. L. Finney, B. Frewen, R. Kern, D. L. Tabb, D. C. Liebler, M. J. MacCoss, *Bioinformatics* **2010**, *26*, 966.

[30] L. Shervington, H. Patil, A. Shervington, *J. Cancer* **2015**, *6*, 786.

[31] T. Maehana, T. Tanaka, H. Kitamura, N. Fukuzawa, H. Ishida, H. Harada, K. Tanabe, N. Masumori, *PLoS One* **2016**, *11*, e0162942.

[32] K. Saito, K. Kukita, G. Kutomi, H. Okuya, H. Asanuma, T. Tabeya, Y. Naishiro, M. Yamamoto, H. Takahashi, T. Torigoe, A. Nakai, Y. Shinomura, N. Hirata, N. Sato, Y. Tamura, *Eur. J. Immunol.* **2015**, *45*, 2028.

[33] E. Ersvaer, A. K. Brenner, K. Vetas, H. Reikvam, O. Bruserud, *BMC Pharmacol. Toxicol.* **2015**, *16*, 12.

[34] B. C. Searle, *Proteomics* **2010**, *10*, 1265.

[35] B. Basiri, M. G. Bartlett, *Bioanalysis* **2014**, *6*, 1525.

[36] D. M. Peng, R. Punn, K. Maeda, E. S. Selamet Tierney, *Ann. Thorac. Surg.* **2016**, *101*, 1005–1010.

[37] C. F. Tsai, Y. T. Wang, H. Y. Yen, C. C. Tsou, W. C. Ku, P. Y. Lin, H. Y. Chen, A. I. Nesvizhskii, Y. Ishihama, Y. J. Chen, *Nat. Commun.* **2015**, *6*, 6622.

[38] K. T. Rigbolt, T. A. Prokhorova, V. Akimov, J. Henningsen, P. T. Johansen, I. Kratchmarova, M. Kassem, M. Mann, J. V. Olsen, B. Blagoev, *Sci. Signal* **2011**, *4*, rs3.

[39] A. N. Kettenbach, D. K. Schweppe, B. K. Faherty, D. Pechenick, A. A. Pletnev, S. A. Gerber, *Sci. Signal* **2011**, *4*, rs5.